Int. J. Electrochem. Sci., 9 **(2014)** 1506 - 1521

International Journal of
ELECTROCHEMICAL
SCIENCE
www.electrochemsci.org

Effect of Harmal Extract on the Corrosion of C-steel in Hydrochloric Solution

L. Bammou[1], M. Belkhaouda[1], R. Salghi[1,], O. Benali[2], A. Zarrouk[3], S. S. Al-Deyab[4], I. Warad[4], H. Zarrok[5], B. Hammouti [3,4]*

[1] Equipe de Génie de l'Environnement et de Biotechnologie, ENSA, Université Ibn Zohr, BP 1136, Agadir, Morocco
[2] Department of Biology, Faculty of Sciences and technology, Saïda University, Algeria
[3] LCAE-URAC18, Faculté des Sciences, Université Mohammed Premier, BP 4808, Oujda,Morocco.
[4] Department of Chemistry, College of Science, King Saud University, B.O. 2455, Riaydh 11451, Saudi Arabia
[5] Laboratoire des procèdes de séparation, Faculté des Sciences, Université Ibn Tofail, Kénitra, Morocco.
[*]E-mail: r.salghi@uiz.ac.ma

Received: 1 May 2013 / *Accepted:* 19 November 2013 / *Published:* 5 January 2014

The extract of harmal (HE) in aqueous 1 M HCl was systematically investigated to ascertain its inhibitor y effect on corrosion of C-steel and its mechanism of the inhibition by electrochemical and weight loss methods.The inhibition efficiency of harmal extract (HE) on corrosion of C-steel in 1 M HCl solution ion increases on increasing in its concentration and decreases with rise in temperature. Potentiodynamic polarization measurement show that HE acts as cathodic type inhibitor. The increase in activation in energies of corrosion process in presence of the extract indicates that HE retarded the rate of corrosion of C-steel in 1 M HCl solution. The nature of adsorption of the extract on C-steel surface was in conformity with Langmuir isotherm. The results obtained with different method are in good agreement. Scanning electron microscopy (SEM) study confirmed that the inhibition of corrosion of C-steel is through adsorption of the extract molecules on surface of metal.

Keywords: C-steel; EIS; polarization; SEM; Harmal extra; inhibition corrosion.

1. INTRODUCTION

The study of carbon steel corrosion phenomena has become important particularly in acidic media because of the increased industrial applications of acid solutions. Hydrochloric acid solutions are widely used for the pickling, cleaning, descaling and etching of mild steel [1-3]. Several authors reported that mixtures of nitrogen and sulphur compounds are often better than either type alone. The

corrosion inhibition efficiency of various organic compounds on the corrosion of steel has been investigated, experimentally [4-19].

The toxicity may manifest either during the synthesis of the compound or during its applications. These lead investigations to focus on the use of naturally occurring substances in order to find low-cost and non-hazardous inhibitors.

Recently, several researcher focalize their works to use of natural products named green inhibitor, as corrosion inhibitors [20-30]. Among these compounds was tested in our laboratory, we cite extract compounds such as; Verbena extract [31], Chamomile extract [32], *Marrubium Vulgare L*. Extract[33], Argan extract [34-36]. These compounds tested have been reported to be excellent inhibitors for metals and alloys in acidic solutions.

In the present work, inhibitive action of harmal extact (**HE**) as a cheap, eco-friendly and naturally occurring substance on corrosion behavior of carbon steel in 1M HCl has been investigated through weight loss and potentiodynamic polarization measurements.

2. EXPERIMENTAL

C-steel specimens used for the study having the composition given in Table 1.

Table 1. Chemical composition of C-steel

Element	C	Si	Mn	Cu	S	Fe
Weight %	0.179	0.165	0.439	0.203	0.034	Balance

The aggressive solution of 1M HCl was prepared by dilution of analytical grade 37% HCl with double distilled water. All experiments were carried out in molar hydrochloric acid solution in the absence and presence of different concentrations **(**0.5, 1, 2 and 4 g/l) of harmal extract (**HE**). The cross section of the working electrode (0.32 cm^2 area) was mechanically ground with emery paper up to 1200 grade, degreased in acetone and rinsed with bidistilled water before immersed in the test solution.

Polarisation measurements and EIS measurements were carried out in a conventional three-electrode electrolytic cell. Saturated calomel electrode (SCE) and platinum electrode were used as reference and auxiliary electrodes respectively.

Gravimetric measurements were carried out in a double walled glass cell equipped with a thermostat cooling condenser. The C-steel specimens of size 2cm×1cm×0.3cm in 1M of hydrochloric acid containing different concentrations of harmal extract at 25°C for 6 h. The solution volume was 100 ml.

A Potentiodynamic polarization measurement was carried out using Voltalab PGZ 100 piloted by ordinate associated to "Volta Master 4" software. The scan rate was 60 mV/min started from an initial potential of -700 to -300 mV/SCE. Before recording each curve, the working electrode is maintained with its free potential of corrosion during 30 minutes.

All experiments were repeated three times at temperature desired ±1°C. Corrosion current densities were obtained from the polarization curves by linear extrapolation of the Tafel curves.

Electrochemical impedance spectroscopy (EIS) was carried out with a same equipment was used as for the Tafel polarization measurements, leaving the frequency response analyser out of consideration.

Quasi-potentiostatic polarization curves were obtained using a sweep rate of 1 mVs^{-1}. After the determination of steady-state current at a given potential, sine wave voltage (10 mV) peak to peak, at frequencies between 100 kHz and 10 mHz were superimposed on the rest potential. Computer programs automatically controlled the measurements performed at rest potential after 30 min of exposure. All potentials were reported versus saturated calomel electrode (SCE). The impedance diagrams are given in the Nyquist representation. Experiments are repeated three times to ensure the reproducibility.

Immersion corrosion analysis of C-steel samples in the acidic solutions with and without the optimal concentration of the inhibitor was performed using SEM. Immediately after the corrosion tests, the samples were subjected to SEM studies to know the surface morphology using SEM Jeol JSM-5800 scanning electron microscope.

3. RESULTS AND DISCUSSION

3.1. Electrochemical measurements

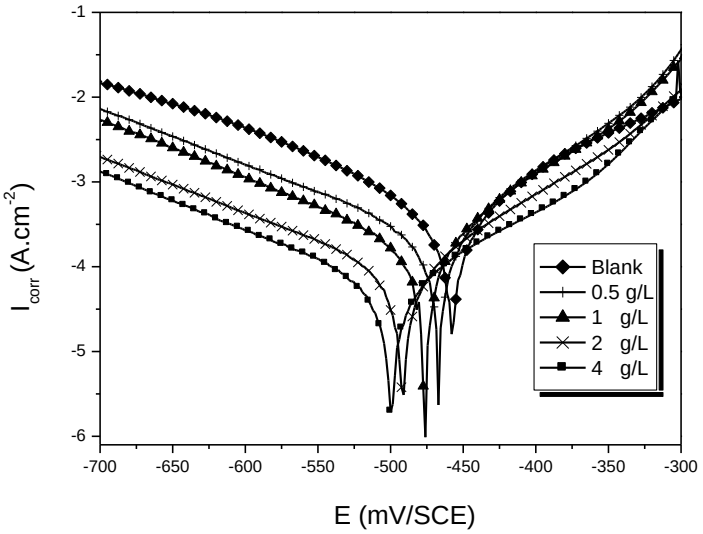

Figure 1. Polarization curves for C-steel in 1M HCl at various concentrations of **HE** at 25°C.

Potentiodynamic anodic and cathodic polarization scans were carried out at 25 °C in 1 M HCl with different concentrations of **HE**. Anodic and cathodic polarization curves in the absence and in the

presence of inhibitor at different concentrations after 0.5 h of immersion and at 25°C are shown in Figure 1.

The corrosion parameters including corrosion current densities (I_{corr}), corrosion potential (E_{corr}), cathodic Tafel slope (b_c), anodic Tafel slop (b_a) and inhibition efficiency (E_I %) are listed in table 2. In the case of polarization method the relation determines the inhibition efficiency (E_I %).

$$E_I\,(\%) = \frac{I_u - I_i}{I_u} \text{x}100 \qquad (1)$$

where I_u is the corrosion current density in uninhibited acid and I_i is the corrosion current density in inhibited acid.

From electrochemical polarization measurements, it is clear from the results that the addition of inhibitor causes a decrease of the current density. The values I_{corr} of C-steel in the inhibited solution are smaller than that for the inhibitor free solution (table 2).

This decrease can be explained by the inhibitory action of this inhibitor. The parallel cathodic Tafel plots obtained in Fig. 1 indicate that the hydrogen evolution is activation-controlled and the slight change of both β_a and β_c indicates that the reduction mechanism is not affected by the presence of inhibitor. In the domain anodic, the polarization curves of C-steel have shown that the addition of the **HE** decreases the current density and moves the corrosion potential to negative values acting mainly on the dissolution reaction of metal. The inhibition efficiency (E_I %) increases with inhibitor concentration reaching 91.08 % at 4 g/L.

However, for anodic polarization, it can be seen from figure 1 that, in the presence of **HE** at majority of concentrations, two linear portions were observed. When the anodic potentials increases, the anodic current increases at a slope of b_{a1} in the low polarization potential region, after passing a certain potential E_u, the anodic current increases rapidly and dissolves at a slope of b_{a2} in the high polarization region. The rapid increase of anodic current after E_u may be due to desorption of **HE** molecules adsorbed on the electrode.

Table 2. Electrochemical parameters for C-steel in 1M HCl at various concentrations of **HE** at 25°C.

Conc. (g/L)	I_{corr} ($\mu A/cm^2$)	E_{corr} (mV/CSE)	β_c (mV/dec)	β_a (mV/dec)	E_I (%)
Blank	594	-457	-204	72	-----
0.5	250	-467	-156	78	57.91
1.0	188	-473	-152	72	68.35
2.0	98	-491	-155	73	83.50
4.0	53	-501	-152	87	91.08

This means that the inhibition mode of **HE** extract depends on electrode potential. In this case, the observed inhibition phenomenon is generally described as corrosion inhibition of the interface associated with the formation of a bidimensional layer of adsorbed inhibitor species at the electrode surface [37-39]. Note that the potential E_u is also denoted E_1 in Bartos and Hackerman's paper [40].

On the other hand, the corrosion rate can be calculated using equation [41-42]:

$$v_{corr}(mm/y) = \frac{3270 \times M \times I_{corr}}{\rho \times Z} \quad (2)$$

Where 3270 is a constant that defines the unit of corrosion rate, I_{corr} is the corrosion current density in A cm^{-2}, ρ is the density of the corroding material (g cm^{-3}), M is the atomic mass of the metal and *Z* is the number of electrons transferred per atom.

Too, in this work we have also tried to calculate polarization resistance from the measurements of corrosion currents using the Stern – Geary equation [43]:

$$R_P = \frac{1}{2.303\, I_{corr}} \times \frac{\beta_a \times \beta_c}{\beta_a + \beta_c} \quad (3)$$

where β_a and β_c are the anodic and cathodic Tafel slopes, respectively.

The corresponding corrosion rate and polarization resistance (R_p) values of C-steel in the absence and in the presence of different inhibitor concentrations are given in table 3. It is apparent that R_p increases with increasing inhibitor concentration. The inhibition percentage (P %) calculated from R_p values are also presented in table 3.

Table 3. Values of corrosion rate and R_p for C-steel in 1M HCl at various concentrations of **HE**.

Conc. (g/L)	V_{corr} (mm/y)	R_p ($\Omega.cm^2$)	E_R (%)
Blank	6.92	38.90	-----
0.50	2.91	90.31	56.92
1	2.19	112.78	65.50
2	1.14	220.47	82.36
4	0.62	452.32	91.40

We remark that E_R % increases with increasing concentration of inhibitor. The inhibition efficiency of corrosion of C-steel is calculated by polarization resistance as follows:

$$E_R(\%) = \frac{R'_p - R_p}{R'_p} \times 100 \quad (4)$$

where R_p and R'_p are the polarization resistance values without and with inhibitor, respectively.

Nyquist plots of C-steel in 1 M HCl in the presence and absence of additive are given in Figure 2. These curves have obtained after 0.5 h of immersion in the corresponding solution. All the plots display a single capacitive loop. Impedance parameters derived from the Nyquist plots, percent inhibition efficiencies, P (%) and the equivalent circuit diagram are given in table 4 and Figure 3, respectively.

The circuit consists of a constant phase element (CPE) Q, in parallel with a resistor R_t The use of CPE-type impedance has been extensively described in [44-47]:

$$Z_{CPE} = \left[Q(jw)^n\right]^{-1} \quad (5)$$

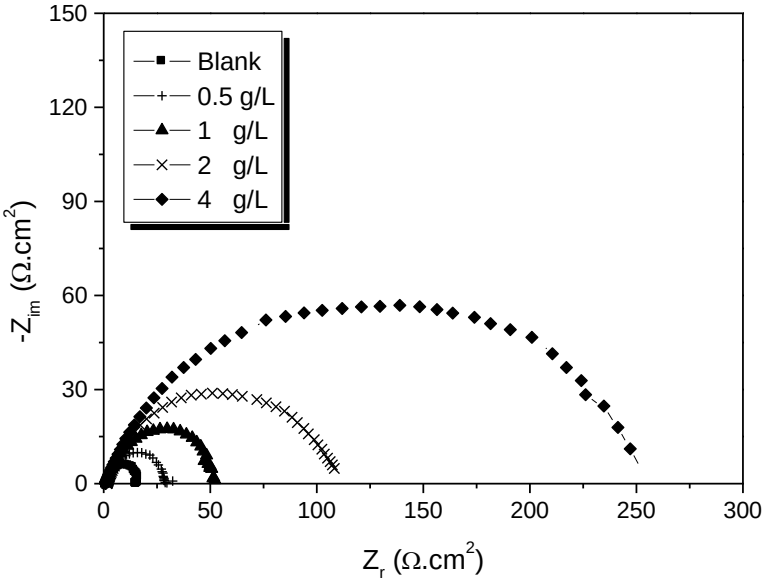

Figure 2. Nyquist plots of C-steel in 1 M HCl without and with different concentrations of HE at at 25°C

Table 4. Impedance parameters for corrosion of steel in 1M HCl without and with different concentrations of **HE** at 25°C

Conc. (g/L)	R_t (Ω.cm²)	Q (S^n/ Ω.cm²)	n	C_{dl} (μF.cm^{-2})	E_{Rt} (%)
Blank	26.00	1.52 x10^{-4}	0.86	62	-----
0.50	34.00	1.67 x10^{-4}	0.83	58	55.88
1.00	51.72	1.36 x10^{-4}	0.85	57	71.01
2.00	83.33	1.25 x10^{-4}	0.84	52	81.76
4.00	214.28	1.02 x10^{-4}	0.83	47	93.20

The above equation provides information about the degree of non-ideality in capacitance behavior. Its value makes it possible to differentiate between the behavior of an ideal capacitor (n = 1) and of a CPE (n < 1).

The percent inhibition efficiency is calculated by charge transfer resistance obtained from Nyquist plots, according to the equation:

$$P\ \% = \frac{R'_t - R_t}{R'_t} \times 100 \qquad (6)$$

where R_t and R'_t are the charge transfer resistance values without and with inhibitor, respectively.

Considering that a CPE may be considered as a parallel combination of a pure capacitor and a resistor that is inversely proportional to the angular frequency, the value of capacitance, C_{dl}, can thus

be calculated for a parallel circuit composed of a CPE (Q) and a resistor (R_t), according to the following formula [48-49]:

$$Q = \frac{(C R_t)^n}{R_t} \quad (7)$$

Generally, Fig. 2 showed that the impedance spectra exhibit one single depressed semicircle, and the diameters of semicircle increases with the inhibitor concentration. The single semicircle can be attributed to the charge transfer that takes place at electrode/solution interface, and the transfer process controls the corrosion reaction of C-steel and the presence of inhibitor does not change the mechanism of dissolution of C-steel [50].

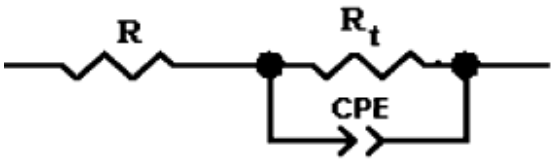

Figure 3. The equivalent circuit of the impedance spectra obtained for **HE**

It is also clear that these impedance diagrams consist of one large capacitive loop and they are not perfect semicircles and this difference has been attributed to frequency dispersion [51-52] and the heterogeneity of the metal surface [53-54].

From table 4, it is clear that the R_t values increase with inhibitor concentration and consequently the inhibition efficiency increases to 93.20 % at 4 g/L. In fact, the presence of **HE** is accompanied by the increase of the value of R_t in acidic solution confirming a charge-transfer process mainly controlling the corrosion of C-steel. Values of double-layer capacitance are also brought down to the maximum extent in the presence of inhibitor and the decrease in the values of C_{dl}. The decrease in C_{dl} is due to the adsorption of the inhibitor on the metal surface leading to the formation of film or complex from acidic solution [55].

A quick examination of the electrochemical and EIS parameters indicates that the values of the corrosion potential, anodic and cathodic Tafel slopes vary slightly in the presence of HE concentration. These results suggest that the action of molecules of **HE** act by pure geometric blocking of the electrode surface.

3.2. Weight loss tests

Values of the inhibition efficiency and corrosion rate obtained from the weight loss measurements of C-steel for different concentrations of **HE** in 1 M HCl at 25 °C after 6 h of immersion are given in table 5. The inhibition efficiency is defined as follows:

$$P\ \% = \frac{W - W'}{W} \times 100 \quad (8)$$

where W and W' are the corrosion rates of C-steel due to the dissolution in 1 M HCl in the absence and the presence of definite concentration of inhibitor, respectively.

Table 5. C-steel weight loss data and inhibition efficiency of **HE**

Conc. (g/L)	W ($mg/h.cm^2$)	Ew (%)
Blank	1.55	-----
0.50	0.71	54.19
1.00	0.50	67.74
2.00	0.24	84.51
4.00	0.16	89.68

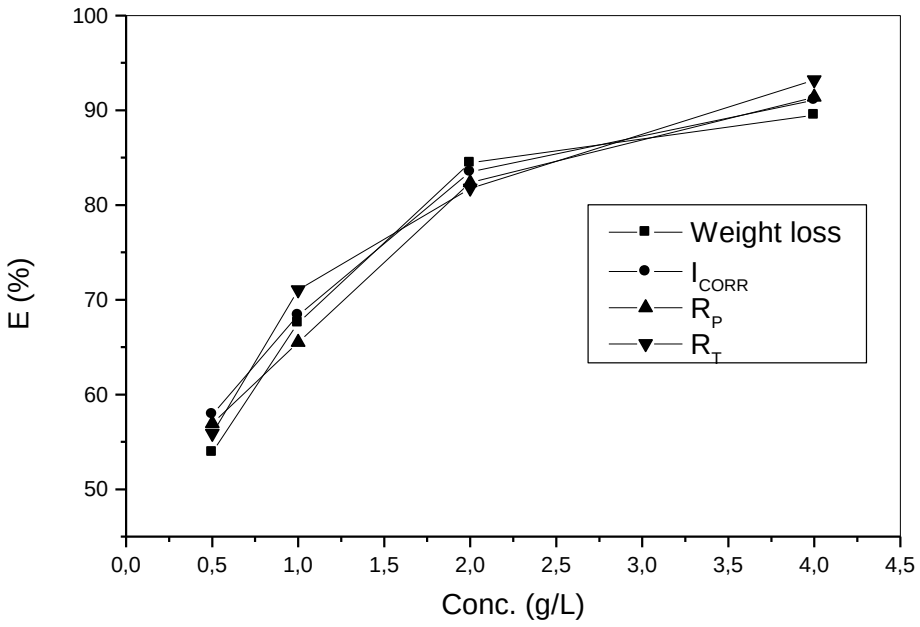

Figure 4. Variation of P % evaluated by different methods

The analysis of these results (Table 5) shows clearly that the corrosion rate decreases (W ($mg/h.cm^2$) while the inhibition efficiency (E_w %) increases with increasing inhibitor concentration reaching a maximum value of 89.68 % at a concentration of 4 g/L. This behavior can be attributed to the increase of the surface covered θ (E_w %/100), and that due to the adsorption of natural compounds on the surface of the metal, as the inhibitor concentration increases. We can conclude that **HE** is a good corrosion inhibitor for C-steel in 1 M HCl solution.

Globally, the inhibition efficiency measured for different methods was estimated at about 90 % and the inhibition efficiency obtained from weight loss and electrochemical measurements are in good agreement (Figure 4).

3.3. Adsorption isotherm and thermodynamic activation parameters

It is well established that the first step in corrosion inhibition of metals and alloys is the adsorption of organic inhibitor molecules at the metal/solution interface and that the adsorption depends on the molecule's chemical composition, the temperature and the electrochemical potential at the metal/solution interface. In fact, the solvent water molecules could also adsorb at metal/solution interface. So the adsorption of organic inhibitor molecules from the aqueous solution can be regarded as a quasi-substitution process between the organic compounds in the aqueous phase [$Org_{(sol)}$] and water molecules at the electrode surface [$H_2O_{(ads)}$] [45]:

$$Org_{(sol)} + nH_2O_{(ads)} \Leftrightarrow Org_{(ads)} + nH_2O_{(sol)} \quad (9)$$

where $Org_{(sol)}$ and $Org_{(ads)}$ are the organic specie dissolved in the aqueous solution and adsorbed onto the metallic surface, respectively, $H_2O_{(ads)}$ is the water molecule adsorbed on the metallic surface and n is the size ratio representing the number of water molecules replaced by one organic adsorbate. Basic information on the adsorption of inhibitors on the metal surface can be provided by adsorption isotherm. In order to obtain the isotherm, the fractional surface coverage values (θ) as a function of inhibitor concentration must be obtained. The values of θ can be easily determined from the weight loss measurements by the ratio E_W % / 100, where E_W% is inhibition efficiency obtained by weight loss method. So it is necessary to determine empirically which isotherm fits best to the adsorption of inhibitor on the steel surface. Several adsorption isotherms (viz., Frumkin, Langmuir, Temkin, Freundlich) were tested and the Langmuir adsorption isotherm was found to provide the best description of the adsorption behaviour of this inhibitor. The Langmuir isotherm is given by following equation:

$$\frac{C}{\theta} = \frac{1}{K} + C \quad (10)$$

Where C is the concentration of inhibitor, K_{ads} is the equilibrium constant of the adsorption process, and θ is the surface coverage.

Plot C/θ versus C yields a straight line (Fig. 5) with regression coefficient almost equal to 1. This suggests that exract in present study obeyed the Langmuir isotherm and there is negligible interaction between the adsorbed molecules.

Generally, the corrosion rate of C-steel in acidic solution increase with the rise of temperature. This is due to the decrease of hydrogen evolution overpotential [39, 56]. In order to understand more about the performance of **HE** with the nature of adsorption and activation processes, the effect of temperature is studied. For this purpose, the potentiodynamic polarization are being employed with the

range of temperature 25-55°C for 30 min of immersion, in the absence and presence of 4 g/L of inhibitor (Figs. 6 and 7). Corresponding data are given in Table 6.

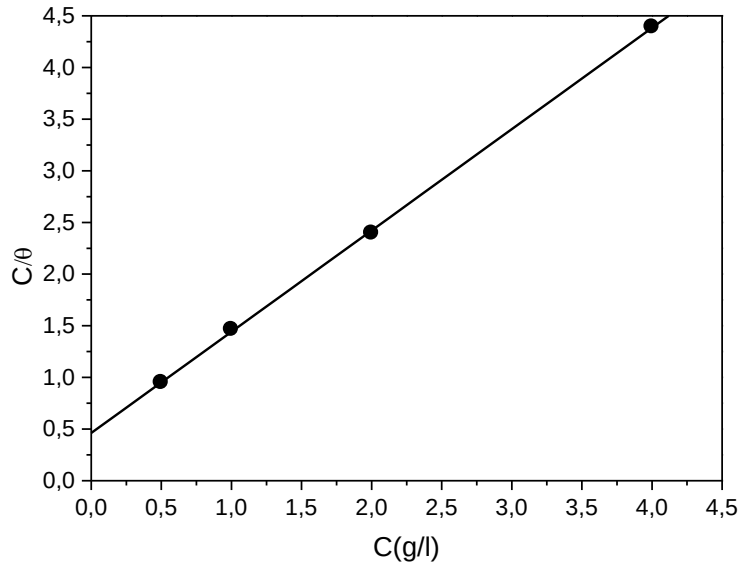

Figure 5. Langmuir isotherm adsorption of **HE** on the C-steel electrode in 1M HCl.

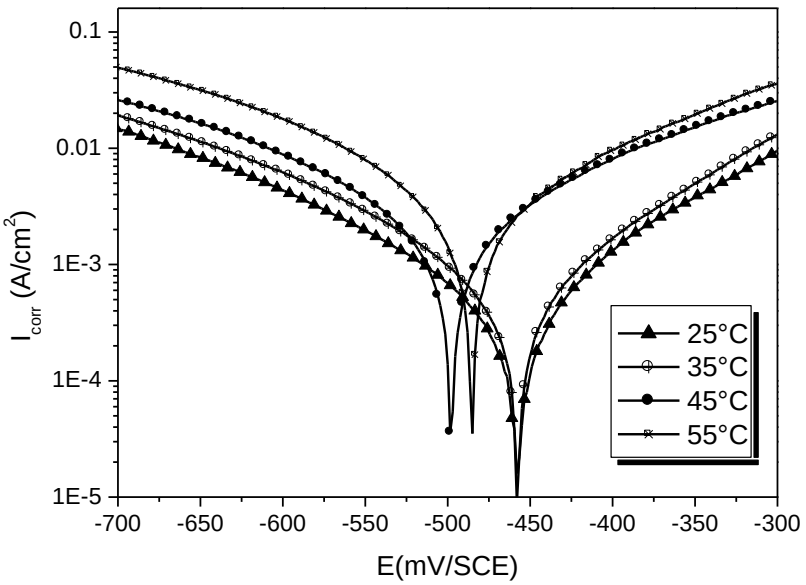

Figure 6. Polarisation curves for C-steel in 1M HCl at different temperature

It's has been observed that the corrosion current density (I_{corr}) increased with the increase in the temperature in the abcense and in the presence of the **HE**. It is seen also that the Harmal extract

investigated have been inhibiting properties at all temperatures studied and the values of inhibition efficiency decreases with temperature increase.

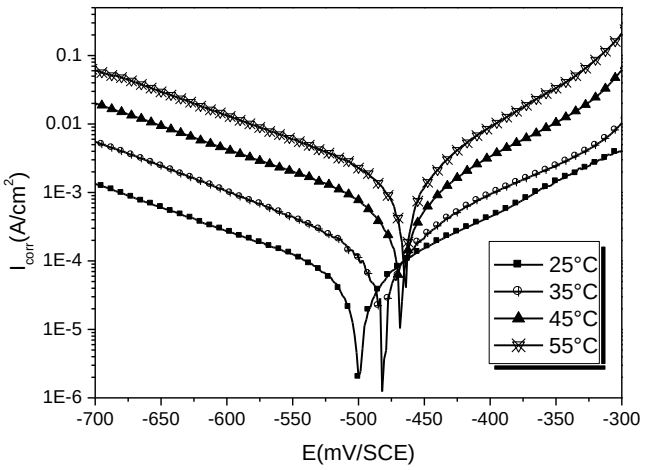

Figure 7. Polarisation curves for C-steel in 1M HCl + 4g/L **HE** at different temperature.

Table 6. Electrochemical parameters for corrosion of C-steel in 1M HCl at different temperatures in the absence and presence of 4 g/L **HE**

Conc. (g/L)	T (°C)	I_{corr} (μA/cm^2)	E_{corr} (mV/CSE)	βc (mV/dec)	E (%)
Blank	25	594	-457	-204	------
	35	900	-458	-199	------
	45	3360	-500	-214	------
	55	6830	-487	-234	------
HE	25	57	-499	-143	90.40
	35	138	-483	-141	84.67
	45	560	-469	-143	83.33
	55	1420	-463	-143	79.21

We were interested in exploring the activation energy of the corrosion process and the thermodynamics of adsorption of **HE**. This was accomplished by investigating the temperature dependence of the corrosion current, obtained using Tafel extrapolation method. The corrosion reaction can be regarded as an Arrhenius-type process, the rate is given by:

$$I_{corr} = A\exp\left(\frac{-E_a}{RT}\right) \qquad (11)$$

where E_a is the apparent activation corrosion energy, T is the absolute temperature, k is the Arrhenius pre-exponential constant and R is the universal gas constant. This equation can be used to calculate the E_a values of the corrosion reaction without and with **HE**. Plotting the natural logarithm of

the corrosion current density versus 1/T, the activation energy can be calculated from the slope. The temperature dependence of C-steel dissolution in 1 M HCl and in the presence inhibitor is presented in Figure 8. The calculated values of the apparent activation corrosion energy in the absence and presence of **HE** are listed in the Table 7. All the linear regression coefficients were close to one. The value of E_a found for **HE** is higher than that obtained for 1 M HCl solution. The increase in the apparent activation energy may be interpreted as physical adsorption [57-58].

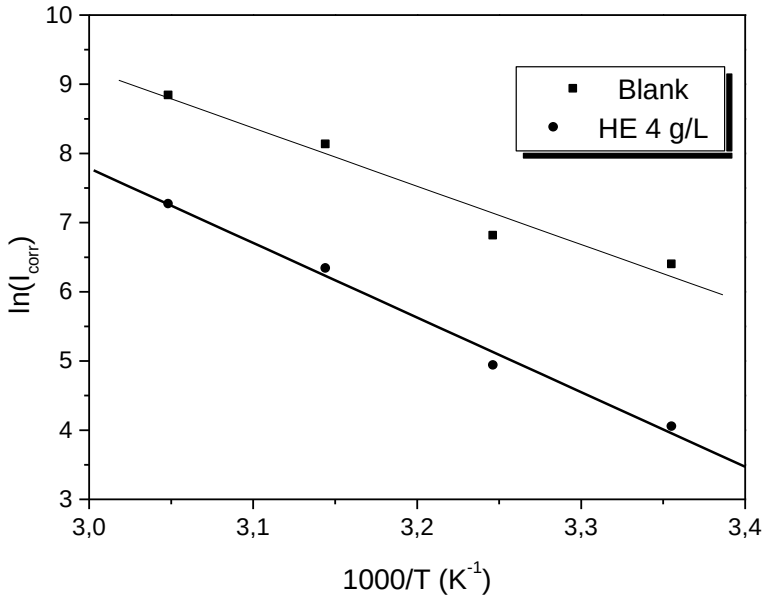

Figure 8. Arrhenius plots of C-steel in 1 M HCl with and without 4 g/L **HE**.

An alternative formulation of Arrhenius equation is [39]:

$$I_{corr} = \frac{RT}{Nh}\exp\left(\frac{\Delta S_a^*}{R}\right)\exp\left(\frac{\Delta H_a^*}{RT}\right) \qquad (12)$$

where *h* is Planck's constant, *N* is Avagadro's number, ΔS_a^* is the entropy of activation and ΔH_a^* is the enthalpy of activation. Figure 9 shows a plot of Ln (I_{corr}/T) vs. 1/T. Straight lines are obtained with a slope of $\frac{\Delta H_a^*}{R}$ and an intercept of Ln R/Nh + $\frac{\Delta S_a^*}{R}$ from which the values of ΔS_a^* and ΔH_a^* are calculated and are given in Table 7.

Table 7. The value of activation parameters for C-steel in 1M HCl in the absence and presence of 4g/l of **HE**.

	E_a (kJ.mol^{-1})	ΔH_a (kJ.mol^{-1})	ΔS_a (J.mol^{-1} .K^{-1})
Blanc	70.04	67.44	-92,62
4 g/L	89.69	87.09	-112,25

Inspection of these data revealed that the thermodynamic parameters (ΔH_a^* and ΔS_a^*) for dissolution reaction of C-steel in 1 M HCl in the presence of inhibitor are higher than that obtained in the absence of inhibitor. The positive sign of ΔH_a^* reflects the endothermic nature of the C-steel dissolution process suggesting that the dissolution of C-steel is slow in the presence of inhibitor [39]. On comparing the values of the entropy of activation ΔS_a^* given in table 7, it is clear that entropy of activation decreases negatively in the presence of **HE** than in the absence of inhibitor, this reflects the formation of an ordered stable layer of inhibitor on the C-steel surface [39, 59].

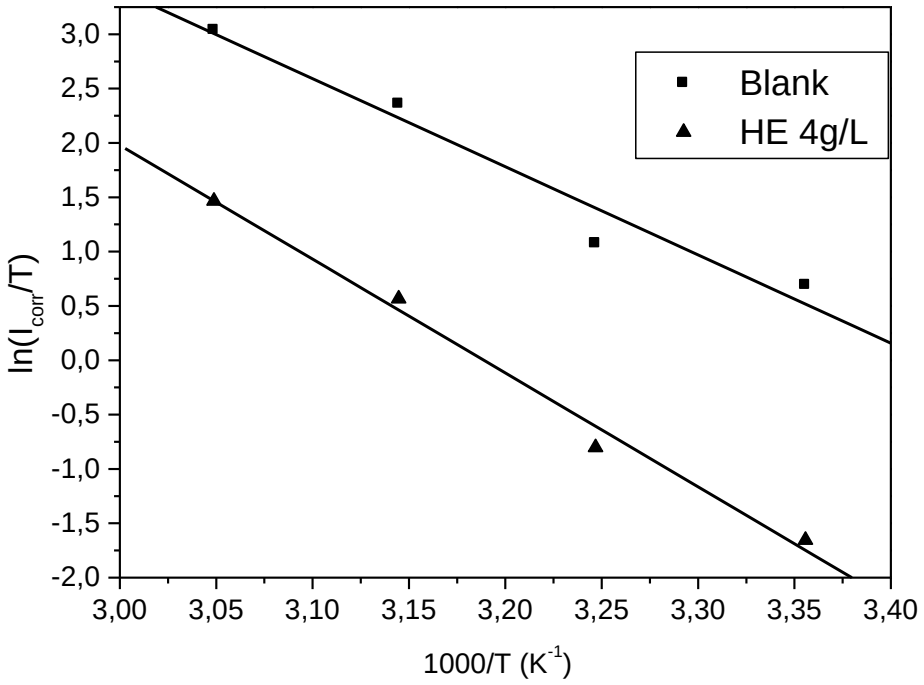

Figure 9. Variation of Ln (Icorr/T) versus 10^3/T for blank and 1M HCl + 4 g/L of **HE**.

3.4. SEM analysis

SEM micrograms of polished surface of C-steel without immersion and exposed for 6 hours in 1 M HCl solutions in absence and presence of 4 grams of **HE** were shown in figure 10(a)-(c). In comparison of SEM micrograms in absence and presence of the extract, there was a rough surface on C-steel in absence of the extract. There was a smooth surface with deposited extract on it in presence of the extract [60]. This result supplements the results of electrochemical techniques and confirms that the **HE** inhibited corrosion of C-steel through adsorption of the inhibitor molecules on metal surface. Examintation of literature showed that the extract contains various components such as β-carboline alkaloids, mostly harmine, as well as harmaline, harmalol, harman, peganine, isopeganine, dipeganine, deoxypeganine and quinazolin derivatives such as vasicine, vasicinone and deoxyvasicinone [61-63].

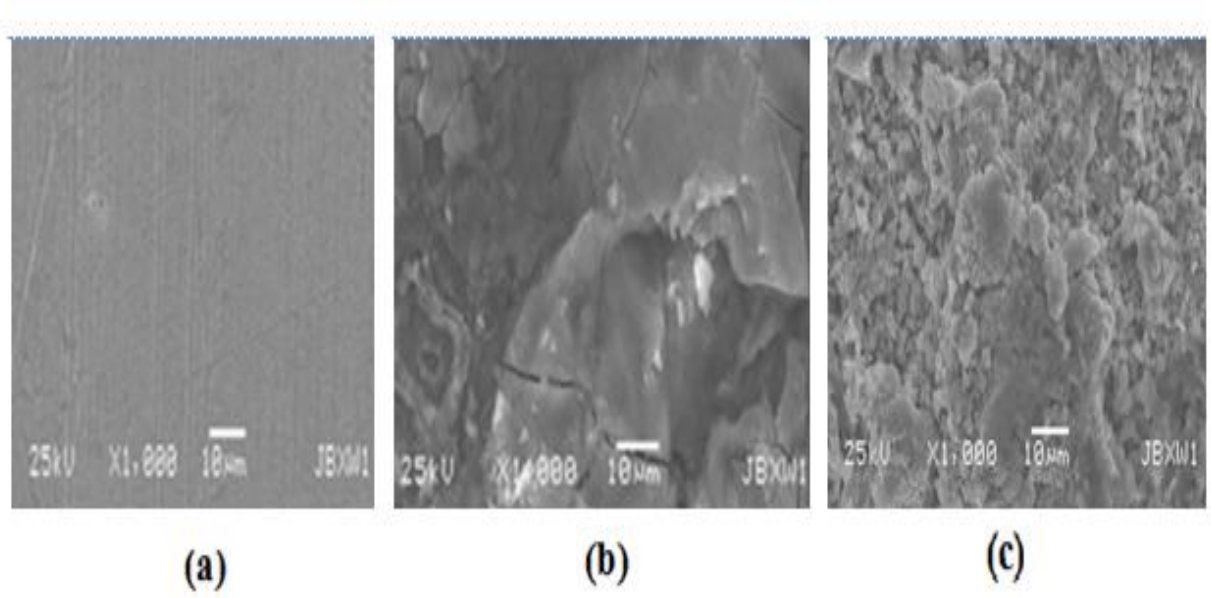

Figure 10. SEM (x1000) of C38 steel **(a)** before immersion **(b)** after 6 hours of immersion in 1.0 M HCl **(c)** after 6 hours of immersion in 1.0 M HCl + 4 g/L of HE.

4. CONCLUSION

Harmal extract (**HE**) examined acted as an efficient corrosion inhibitor in 1 M HCl. Polarization studies showed that **HE** was a cathodic inhibitor and its inhibition efficiency increased with the inhibitor concentration but decreases with rise in temperature. Impedance method indicates that **HE** adsorbs on the C-steel surface with increasing transfer resistance and decreasing of the double-layer capacitance. The adsorption of **HE** on the C-steel in 1 M HCl solution obey Langmuir adsorption isotherm with high correlation coefficient. The adsorption process is a spontaneous and exothermic process. The inhibitor efficiency determined by electrochemical methods and by gravimetric methods are in good agreement. SEM examination of the electrode surface confirmed the existence of such adsorbed film.

ACKNOWLEDGEMENTS
Prof S. S. Deyab, Prof B. Hammouti and Prof R. Salghi extend their appreciation to the Deanship of Scientific Research at King Saud University for funding the work through the research group project No. RGP-VPP-089.

References

1. A. O. James, N. Oforka, K. Abiola Olusegun, *Int. J. Electrochem. Sci.*, 2 (2007) 278.
2. U. J. Ekpe, P. C. Okafor, E. E. Ebenso, O. E. Offiong, B. I. Ita, *Bull. Electrochem.*, 17 (2001) 135.
3. S. A. Odoemelam, N. O. Eddy, *J. Surf. Sci. Technol.*, 24 (2008) 65.
4. H. Zarrok , A. Zarrouk , B. Hammouti, R. Salghi, C. Jama, F. Bentiss , *Corros. Sci.*, 64 (2012) 243.

5. H. Zarrok , H. Oudda , A. Zarrouk , R. Salghi, B. Hammouti, M. Bouachrine, *Der Pharm. Chem.,* 3 (2011) 576.
6. H. Zarrok, R. Salghi, A. Zarrouk, B. Hammouti, H. Oudda, Lh. Bazzi, L. Bammou, S. S. Al-Deyab, *Der Pharm. Chem.*, 4 (2012) 407.
7. H. Zarrok, S. S. Al-Deyab, A. Zarrouk, R. Salghi, B. Hammouti, H. Oudda, M. Bouachrine, F. Bentiss, *Int. J. Electrochem. Sci.,* 7 (2012) 4047.
8. D. Ben Hmamou, R. Salghi, A. Zarrouk, H. Zarrok, B. Hammouti, S. S. Al-Deyab, M. Bouachrine, A. Chakir, M. Zougagh, *Int. J. Electrochem. Sci.*, 7 (2012) 5716.
9. 9. A. Zarrouk, B. Hammouti, S.S. Al-Deyab, R. Salghi, H. Zarrok, C. Jama, F. Bentiss, *Int. J. Electrochem. Sci.*, 7 (2012) 5997.
10. A. Zarrouk, H. Zarrok, R. Salghi, B. Hammouti, S.S. Al-Deyab, R. Touzani, M. Bouachrine, I. Warad, T. B. Hadda, *Int. J. Electrochem. Sci.,* 7 (2012) 6353.
11. A. Zarrouk, M. Messali, H. Zarrok, R. Salghi, A. Al-Sheikh Ali,B. Hammouti, S. S. Al-Deyab, F. Bentiss, *Int. J. Electrochem. Sci.*, 7 (2012) 6998.
12. H. Zarrok, A. Zarrouk, R. Salghi, Y. Ramli, B. Hammouti, S. S. Al-Deyab, E. M. Essassi, H. Oudda, *Int. J. Electrochem. Sci*., 7 (2012) 8958.
13. D. Ben Hmamou, R. Salghi, A. Zarrouk, H. Zarrok, S. S. Al-Deyab, O. Benali, B. Hammouti, *Int. J. Electrochem. Sci.*, 7 (2012) 8988.
14. A. Zarrouk, M. Messali, M. R. Aouad, M. Assouag, H. Zarrok, R. Salghi, B. Hammouti, A. Chetouani, *J. Chem. Pharm. Res.*, 4 (2012) 3427.
15. D. Ben Hmamou, M. R. Aouad, R. Salghi, A. Zarrouk, M. Assouag, O. Benali, M. Messali, H. Zarrok, B. Hammouti, *J. Chem. Pharm. Res.*, 4 (2012) 3489.
16. H. Zarrok, H. Oudda, A. El Midaoui, A. Zarrouk, B. Hammouti, M. Ebn Touhami, A. Attayibat,S. Radi, R. Touzani, *Res. Chem. Intermed.*, (2012) DOI 10.1007/s11164-012-0525-x
17. I.B. Obot, N.O. Obi-Egbedi, N.W. Odozi, *Corros. Sci.*, 52 (2010) 923.
18. V.R. Saliyan, A.V. Adhikari, *Corros. Sci.*, 50 (2008) 55.
19. S.A. Ali, H.A. Al-Muallem, S.U. Rahman, M.T. Saeed, *Corros. Sci.*, 50 (2008) 3070.
20. N. Lahhit, A. Bouyanzer, J.M. Desjobert, B. Hammouti, R. Salghi, J. Costa, C. Jama, F. Bentiss, L. Majidi, *Port. Electrochim Acta.,* 29 (2011) 127.
21. L. Bammou, M. Mihit, R. Salghi, L. Bazzi, A. Bouyanzer, B. Hammouti, *Int. J. Electrochem. Sci*., 6 (2011) 1454.
22. M. Larif, A. Elmidaoui, A. Zarrouk, H. Zarrok, R. Salghi, B. Hammouti, H. Oudda, F. Bentiss, *Res Chem Intermed*., (2012) DOI 10.1007/s11164-012-0788-2.
23. D. Ben Hmamou, R. Salghi, A. Zarrouk, B. Hammouti, S.S. Al-Deyab, Lh. Bazzi, H. Zarrok, A. Chakir, L. Bammou, *Int. J. Electrochem. Sci*., 7 (2012) 2361.
24. D. Ben Hmamou, R. Salghi, A. Zarrouk, O. Benali, F. Fadel, H. Zarrok, and B. Hammouti, *Inter. J. Ind. Chem.,* 3 (2012) 25.
25. D. Ben Hmamou, R. Salghi, A. Zarrouk, H. Zarrouk, M. Errami, B. Hammouti, L. Afia, Lh. Bazzi, L. Bazzi, *Res Chem Intermed*., (2012) DOI 10.1007/s11164-012-0609-7.
26. D. Ben Hmamou, R. Salghi, A. Zarrouk, B. Hammouti, S. S. Al-Deyab, Lh. Bazzi, H. Zarrok, A. Chakir, L. Bammou, *Int. J. Electrochem. Sci*., 7 (2012) 2361.
27. L. Afia, R. Salghi, L. Bammou, El. Bazzi, B. Hammouti, L. Bazzi, A. Bouyanzer, *J. Saudia Chem. Soc*., (2011) DOI.org/10.1016/j.jscs.2011.05.008.
28. L. Afia, R. Salghi, El. Bazzi, L. Bazzi, M. Errami, O. Jbara, S. S. Al-Deyab, B. Hammouti, *Int. J. Electrochem. Sci*., 6 (2011) 5918.
29. N. Lahhit, A. Bouyanzer, J. M. Desjobert, B. Hammouti, R. Salghi, J. Costa, C. Jama, F. Bentiss and L. Majidi, *Port. Electrochim. Acta*., 29 (2011) 127.
30. L. Bammou, B. Chebli, R. Salghi, L. Bazzi, B. Hammouti, M. Mihit and H. El Idrissi, Green. *Chem. Lett. Rev*., 3 (2010) 173.

31. D. Ben Hmamou, R. Salghi, A. Zarrouk, S. S. Al-Deyab, H. Zarrok, B. Hammouti, E. Errami, *Int. J. Electrochem. Sci*., 7 (2012) 6234.
32. D. Ben Hmamou, R. Salghi, A. Zarrouk, M. Messali, H. Zarrok, M. Errami, B. Hammouti, Lh. Bazzi, A. Chakir, *Der Pharm. Chem.*, 4 (2012) 1496.
33. D. Ben Hmamou, R. Salghi, A. Zarrouk, H. Zarrok, O. Benali, M. Errami, B. Hammouti, *Res Chem Intermed*., (2012) DOI 10.1007/s11164-012-0840-2.
34. D. Ben Hmamou, R. Salghi, L. Bazzi, B. Hammouti, S.S. Al-Deyab, L. Bammou, L. Bazzi, A. Bouyanzer, *Int. J. Electrochem. Sci*., 7 (2012) 1303.
35. L. Afia, R. Salghi, L. Bazzi, M. Errami, O. Jbara, S.S. Al-Deyab, B. Hammouti, *Int J Electrochem*. Sci., 6 (2011) 5918.
36. L. Afia, R. Salghi, E. Bazzi, A. Zarrouk, B. Hammouti, M. Bouri, H. Zarrouk, L. Bazzi, L. Bammou. *Res Chem Intermed*., (2012) DOI:10.1007/s11164-012-0496-y
37. W. J. Lorentz, F. Mansfeld, *Corros. Sci.,* 31 (1986) 467.
38. O. Benali, L. Larabi, B. Tabti and Y. Harek, *anti-corr. Meth. mater.*,52 (2005) 280.
39. L. Afia, R. Salghi, A. Zarrouk, H. Zarrok, O. Benali, B. Hammouti, S.S. Al-Deyab, A. Chakir, L. Bazzi, *Port. Electrochim. Acta*, 30 (2012) 267.
40. M. Bartos, N. Hackerman, *J. Electrochem. Soc*., 139 (2000) 3428.
41. Electrochemistry and Corrosion Overview and Techniques, Application Note CORR-4, EG and G, Princeton Applied Research, USA, 2004.
42. G. M. Spinks, A. J. Dominis, G. G. Wallace, D. E. Tallman, *J. Solid State Electrochem.*, 6 (2002) 85.
43. L. Larabi, O. Benali, Y. Harek, *Mater. Lett.,* 61 (2007) 3287.
44. O. Benali, L. Larabi, S. M. Mekelleche, Y. Harek, *J. Mater. Sci.*, 41 (2006) 7064.
45. O. Benali, L. Larabi, Y. Harek, *J. Appl. Electrochem.*, 39 (2009) 769.
46. S. Merah, L. Larabi, O. Benali, Y. Harek, *Pig. Res. Tech.*, 37 (2008) 291.
47. C. Selles, O. Benali, B. Tabti, L. Larabi, Y. Harek, *J. Mater. Environ. Sci.*, 3 (2012) 206.
48. L. Larabi, Y. Harek, O. Benali, S. Ghalem, *Prog. Org. Coat.*, 54 (2005) 256.
49. H. B. Ouici, O. Benali, Y. Harek, L. Larabi, B. Hammouti, A. Guendouzi, *Res. Chem. Intermed.*, (2012) DOI 10.1007/s11164-012-0797-1.
50. M. Znini, L. Majidi, A. Bouyanzer, J. Paolini, J.-M. Desjobert, J. Costa, B. Hammouti, *Arab. J. Chem.,* 5 (2012) 467.
51. F. Mansfeld, M. W. Kending, S. Tsai, *Corrosion*, 37 (1981) 301.
52. F. Mansfeld, M. W. Kending, S. Tsai, *Corrosion,* 38 (1982) 570.
53. K. Juttner, *Electrochim. Acta,* 35 (1990) 1501.
54. T. Pajkosay, *J. Electroanal. Chem.*, 364 (1994) 111.
55. F. Bentiss, M. Lagrenée, M. Traisnel, J. C. Hornez, *Corros. Sci.*, 41 (1999) 789.
56. A. Popova, E. Sokolova, S. Raicheva, M. Christov, *Corros. Sci*., 45 (2003) 33.
57. S. Martinez, I. Stern, *Appl. Surf. Sci*., 199 (2002) 83.
58. T. Szauer, A. Brand, *Electrochim. Acta,* 26 (1981) 1219.
59. A. Yurt, A. Balaban, S.U. Kandemir, G. Bereket, B. Erk, *Mater. Chem. Phys*., 85 (2004) 420.
60. M. Ramananda Singh, *J. Mater. Environ. Sci.*, 4 (2013) 119.
61. J. Asgarpanah, F. Ramezanloo, *Afr. J. Pharm. Pharmacol.*, 6 (2012) 1573
62. F. Fathizad, Y. Azarmi, L. Khodaie, *Iranian J. Pharm. Sci.*, 2 (2007) 81.
63. A. Madadkar Sobhani, S.A. Ebrahimi, M. Mahmoudian, *J. Pharm. Pharmaceut. Sci.*, 5 (2002) 19.